Supporting Information

Skin-inspired laminated liquid metal doped hydrogel with mechanical toughness and high electrical conductivity

Junlong Wang[a], Xiaosheng Huo[a], Wenjun Huang[a], Junbin Xu[b], Pengcheng Yu[b], Xiangqian Zhang[b], Zhenhua Cong[a*], Jian Niu[b*]

a. Nano and Heterogeneous Materials Center, School of Materials Science and Engineering, Nanjing University of Science and Technology, Nanjing, Jiangsu 210094, China.

b. State Key Laboratory for Organic Electronics and Information Displays & Institute of Advanced Materials (IAM), Jiangsu National Synergetic Innovation Center for Advanced Materials (SICAM), Nanjing University of Posts & Telecommunications, Nanjing 210023, China.

*E-mail: zhcong@njust.edu.cn；iamjniu@njupt.edu.cn

The force analysis of LMPs was conducted (simplified to the sedimentation process of uniformly dispersed LMPs in the solution, ignoring the impact of solvent loss). The LMPs are primarily subjected to three forces: their own gravity F_g , the buoyancy F_b exerted by the solution on the LMPs, and the friction F_d during the sedimentation process. The formula for each force is as follows:

The gravity of the LMPs is:

$$F_g = \frac{1}{6}\pi d^3 \rho_{LM} g \quad (1)$$

where d is the diameter of the LMPs, ρ_{LM} is the density of the LMPs, and g is the gravitational acceleration.

The buoyancy of the solution on the LMPs is:

$$F_b = \frac{1}{6}\pi d^3 \rho_{PPS} g \quad (2)$$

where ρ_{PPS} is the density of the PVA-PEDOT:PSS solution.

Due to the viscosity of the liquid, the frictional force experienced by the LMPs during sedimentation in the solution is:

$$F_d = 3\pi d \eta v \quad (3)$$

where η is the viscosity coefficient of the solution and v is the sedimentation velocity of the LMPs. When the LMPs begin to sediment, v is initially small, resulting in a small F_d. As gravity causes v to gradually increase, it eventually reaches a certain value, at which point the LMPs achieve force equilibrium, given by:

$$F_g - F_b - F_d = 0 \quad (4)$$

Substitute equations (1) to (3) into equation (4):

$$\frac{1}{6}\pi d^3 (\rho_{LM} - \rho_{PPS}) g - 3\pi d \eta v = 0 \quad (5)$$

$$v = \frac{(\rho_{LM} - \rho_{PPS})}{18\eta} g d^2 \quad (6)$$

From equation (6), it is evident that the sedimentation velocity of the LMPs is proportional to the square of their diameter.

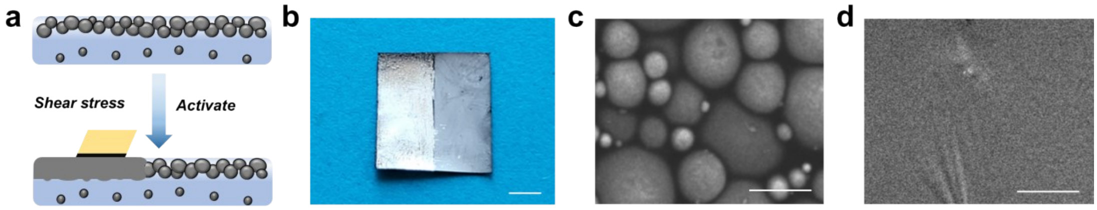

Figure S1. Activation of the LM conductive layer via shear stress.

Figure S2. Resistance values of activated and deactivated parts of $PPS_2LM_{1.5}$ film.

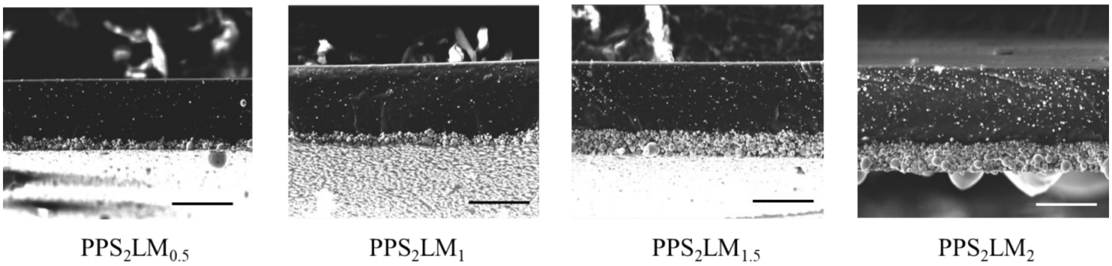

Figure S3. SEM image of cross-section of PPSLM film with different LM contents (Scale: 40 μm).

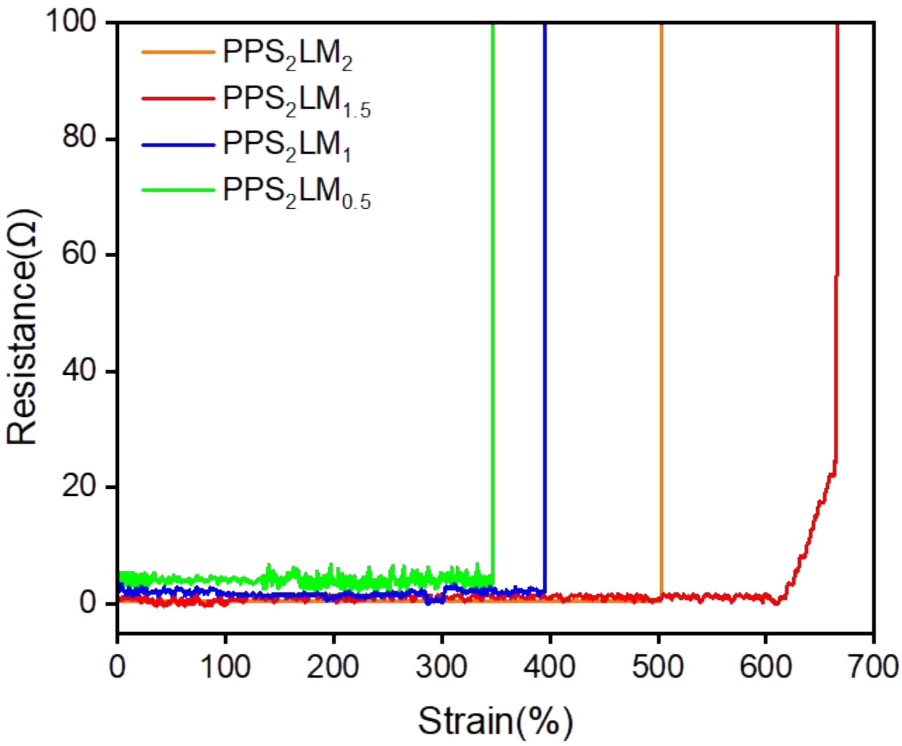

Figure S4. Resistance-Strain curve of PPSLM film with different LM contents.

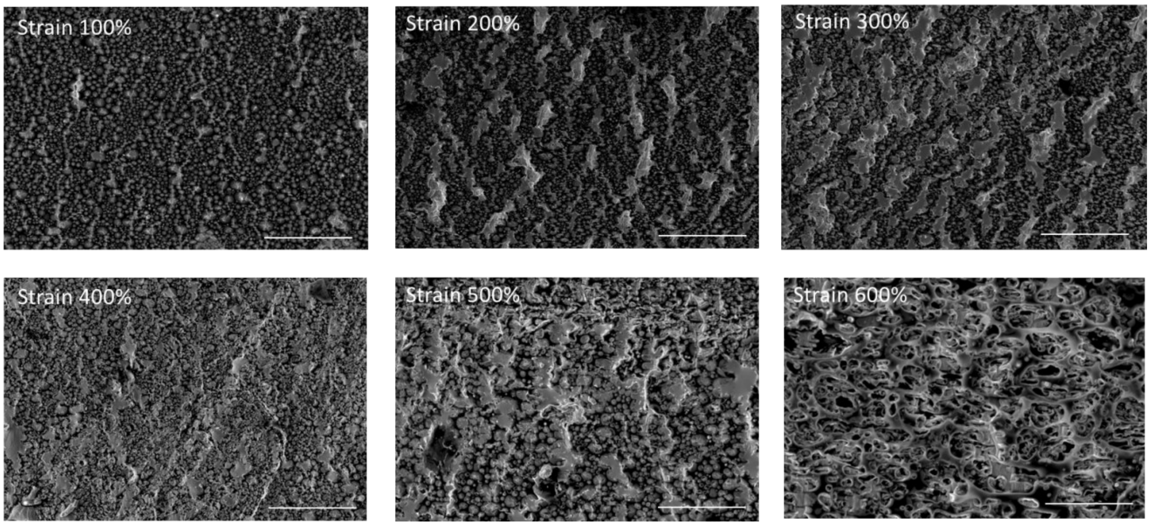

Figuer S5. SEM image of the bottom of the $PPS_2LM_{1.5}$ film under different strain (Scale: 100 μm).

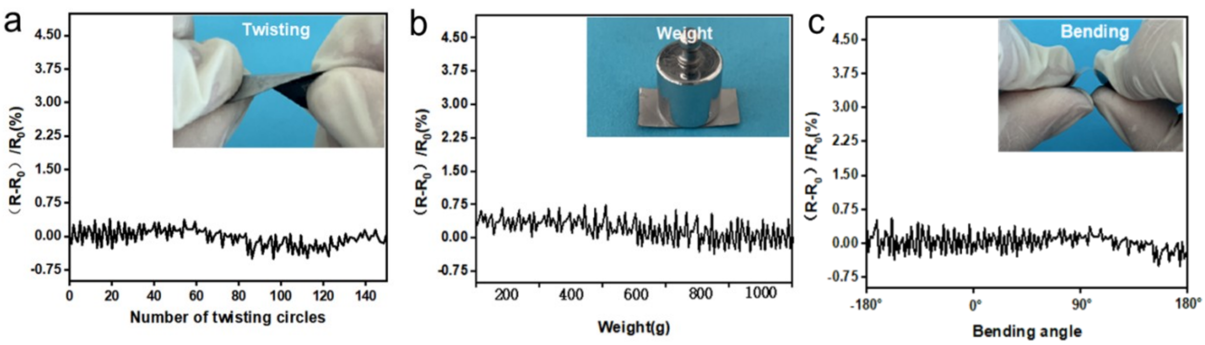

Figure S6. Resistance changes of $PPS_2LM_{1.5}$ film under Torsion a), Pressure b), and Bending c).

Figure S7. $PPS_2LM_{1.5}$ film thickness.

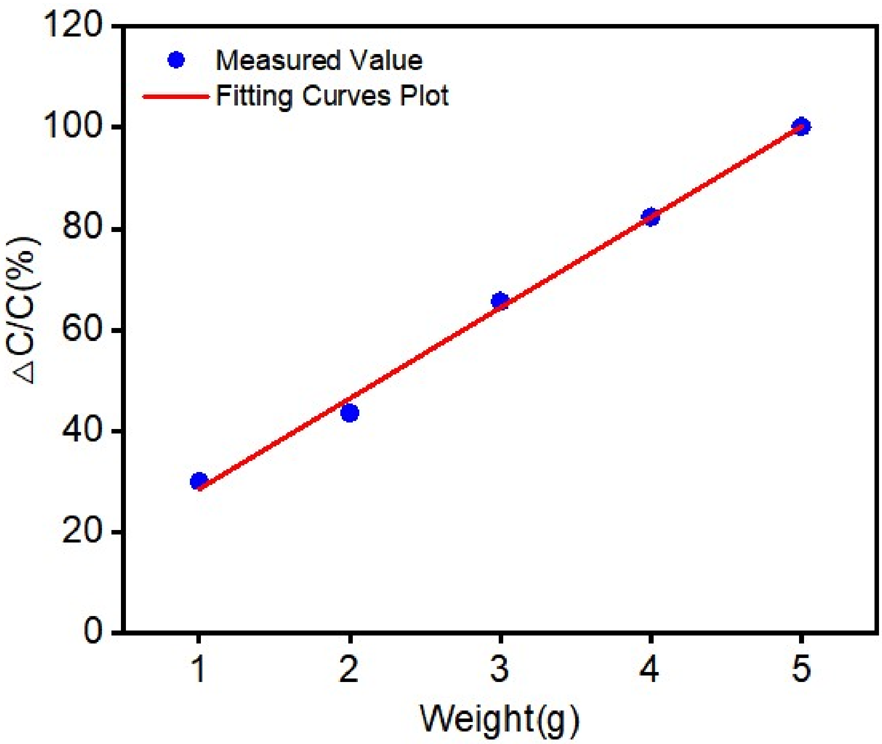

Figure S8. Fitting curve of weight and capacitance response.

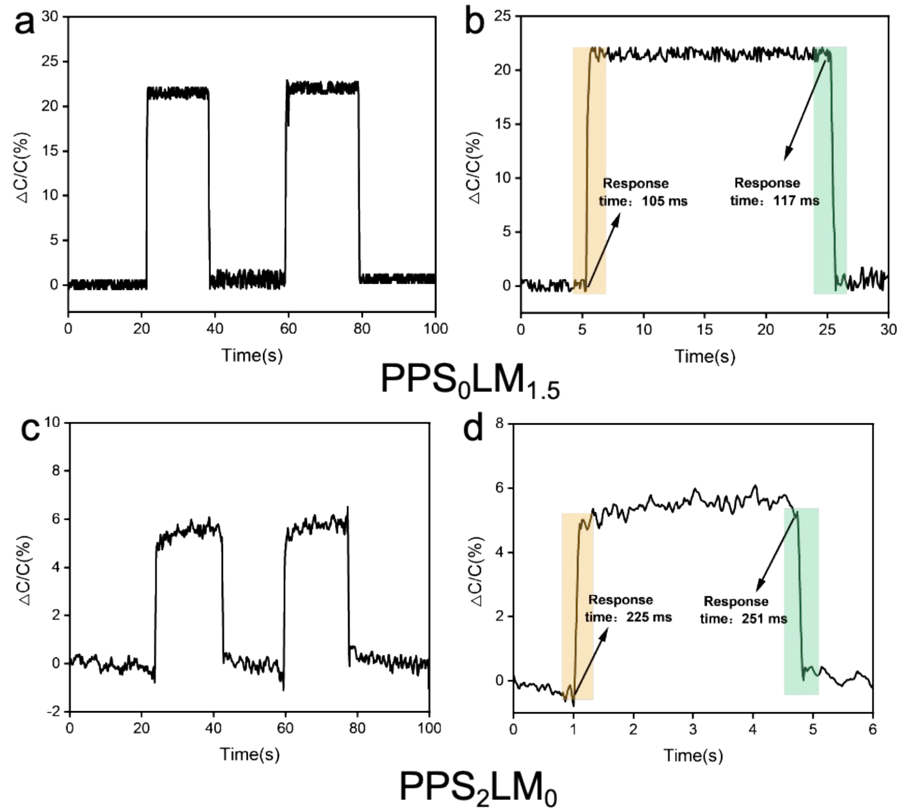

Figure S9. Capacitance response of a sensor based on a, b)$PPS_0LM_{1.5}$ and c, d) PPS_2LM_0 hydrogel films.

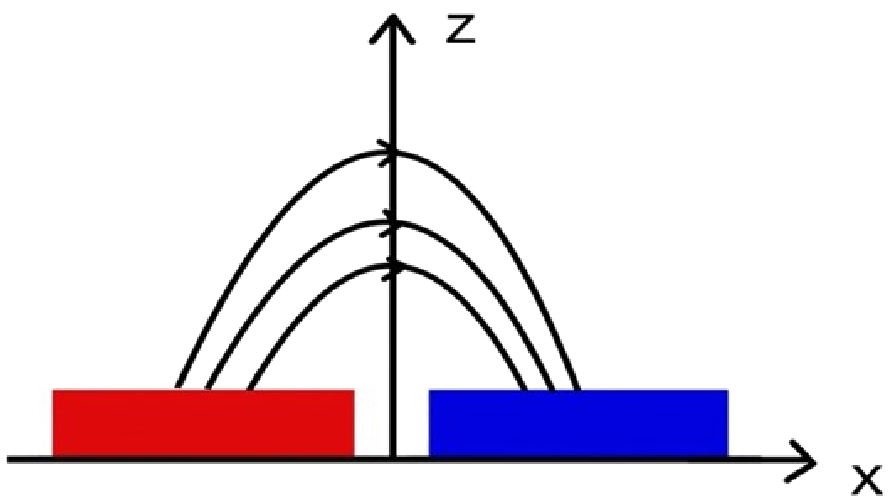

Figure S10. Schematic diagram of electric field lines in crossed finger electrodes.

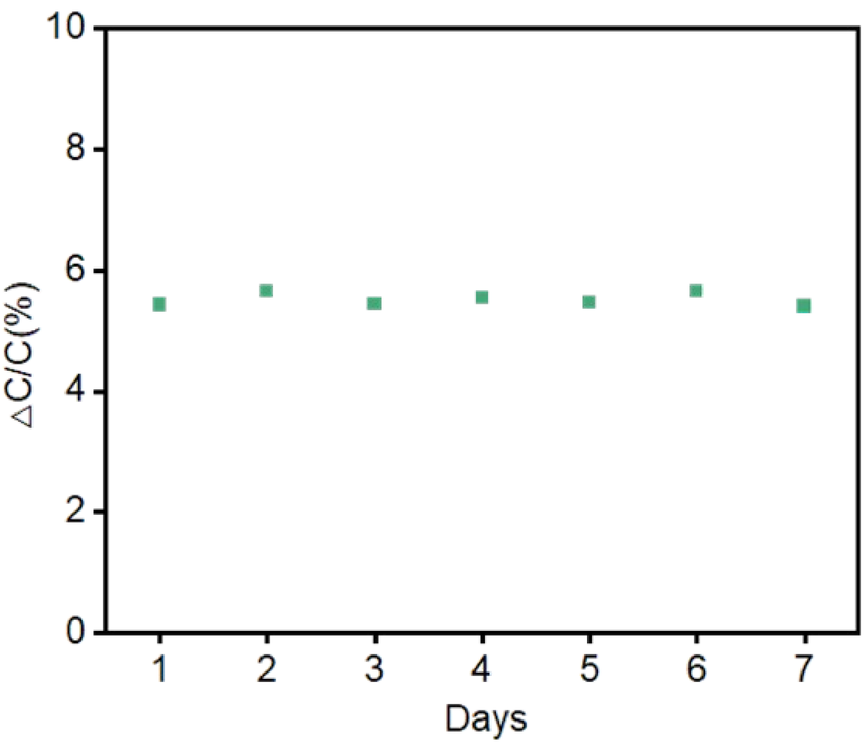

Figure S11. Stability of $PPS_2LM_{1.5}$ contactless capacitive sensor.

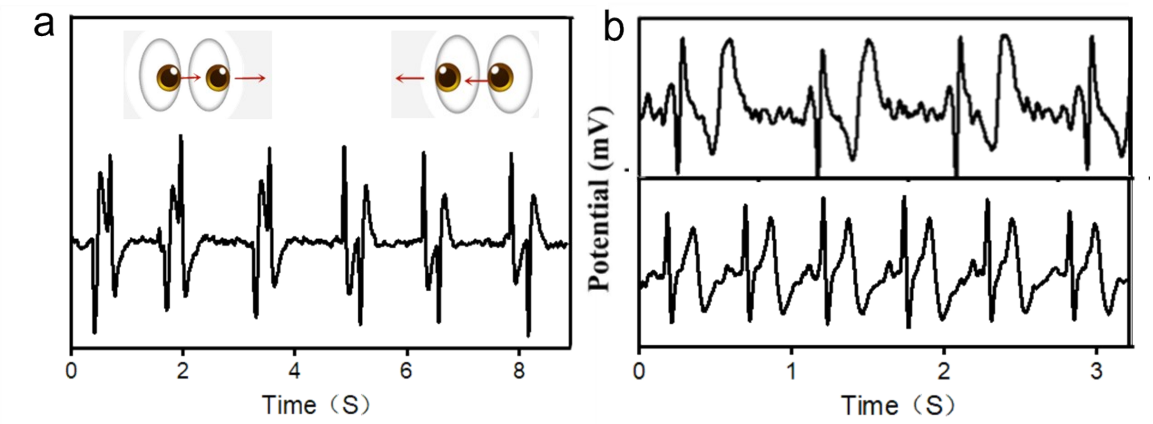

Figure S12. Detection of human bioelectrical signals by $PPS_2LM_{1.5}$ film electrodes. a) Eye signal response. b) Heart signal response before and after exercise.

Table S1. Comparison of our PPSLM hydrogel with some previously reported conductive hydrogels

Materials	Tensile strain	Tensile stress (MPa)	Conductivity (S/m)	Ref.
LM/PEDOT:PSS/PVA (LMPP)	380%	0.088	4.85	1
LM/PAA/PVA	600%	1.5	10.3	2
PVA/EGaInSn–Ni	800%	-	0.04	3
PVA-LMPs	-	-	0.375	4
PEDOT:PSS-PVA	300%	-	-	5
DFS PEDOT:PSS-PVA	600%	0.84	0.32	6
PEDOT:PSS/PVA	150%	0.75	1000	7
LM-CNF-PVA	140%	0.3	3.1×10^5	8
AgNWs-LM-PVA	3000%	33	24	9
PPSLM	818%	24.6	1.67×10^5	This work

Supplementary References

1．K. Zhao, Y. Zhao, J. Xu, R. Qian, Z. Yu, C. Ye, *Chemical Engineering Journal* **2024**, *494*, 152971.

2．J. Zhang, J. Liao, Z. Liu, R. Zhang, M. Sitti, *Adv Funct Materials* **2024**, *34*, 2308238.

3．B. Zhao, Z. Bai, H. Lv, Z. Yan, Y. Du, X. Guo, J. Zhang, L. Wu, J. Deng, D. W. Zhang, R. Che, *Nano-Micro Lett*. **2023**, *15*, 79.

4．M. Liao, H. Liao, J. Ye, P. Wan, L. Zhang, *ACS Appl. Mater. Interfaces* **2019**, *11*, 47358.

5．G. Li, K. Huang, J. Deng, M. Guo, M. Cai, Y. Zhang, C. F. Guo, *Advanced Materials* **2022**, *34*, 2200261.

6．Z. Shen, Z. Zhang, N. Zhang, J. Li, P. Zhou, F. Hu, Y. Rong, B. Lu, G. Gu, *Advanced Materials* **2022**, *34*, 2203650.

7．Z. Zhang, G. Chen, Y. Xue, Q. Duan, X. Liang, T. Lin, Z. Wu, Y. Tan, Q. Zhao, W. Zheng, L. Wang, F. Wang, X. Luo, J. Xu, J. Liu, B. Lu, *Adv Funct Materials* **2023**, *33*, 2305705.

8．X. Li, P. Zhu, S. Zhang, X. Wang, X. Luo, Z. Leng, H. Zhou, Z. Pan, Y. Mao, *ACS Nano* **2022**, **16**, 5909.

9．X. Wang, S. Zheng, J. Xiong, Z. Liu, Q. Li, W. Li, F. Yan, *Advanced Materials* **2024**, 2313845.